Environmental Science
Processes & Impacts

Accepted Manuscript

Environmental impact

Fluorosis is a widespread problem in the Datong Basin, northern China, where groundwater is the most important water supply source for domestic, agricultural, and industrial demands. There are 82,095 and 8,620 people suffering from severe dental and skeletal fluorosis in Shanyin county and Yingxian county, the most seriously fluorosis-affected areas in Datong basin. The hydrochemical characteristics of high fluoride groundwaters and some Factors influencing F levels in sedimentary aquifers in Datong Basin have been investigated by us. In this study, the hydrochemical and isotope investigation was carried out to reveal the water–rock interaction, ion exchange and hydrogeochemical processes of high fluoride groundwater at Datong. The results of this study not only help to understand deeply the genesis of high fluoride groundwater at Datong, but reveal some of the commonly occurring geochemical processes in endemic fluorosis-affected areas in other parts of the world.

Isotope hydrochemical approach to understand fluoride release into groundwaters of Datong Basin, northern China

Chunli Su, Yanxin Wang*, Xianjun Xie, Yapeng Zhu

School of Environmental Studies, China University of Geosciences, 430074 Wuhan, China

*Corresponding author. Tel: +86-27-67883998; Fax: +86-27-87481030; Mail to: yx.wang@cug.edu.cn (Y. Wang)

ABSTRACT: The hydrogeochemical and isotopic investigations of high fluoride (up to 8.26 mg L^{-1}) groundwater in Datong Basin, northern China, were carried in order to evaluate the geochemical controls on fluoride enrichment. The groundwater fluoride concentration tends to increase along with the regional groundwater flow path away from the basin margins, towards the central parts of the basin. Groundwater with high F concentrations has a distinctively major ion chemistry, being generally HCO_3^--rich, Na-rich, Ca-poor, weak alkaline pH values (7.2 to 8.2), and Na–HCO_3 waters. These data indicate that variations in the groundwater major ion chemistry and possibly pH, which are controlled by water–rock interaction processes in the aquifer, are important in mobilizing F. Positive correlations between fluoride with LNa and HCO_3^- in groundwater show that high fluoride content and alkaline sodic characteristics of groundwater result from dissolution of fluorine-bearing minerals. The occurrence and behavior of fluorine in groundwater are mainly controlled by fluorite precipitation as a function of Ca^{2+} concentration. A positive correlation between fluoride and $\delta^{18}O$, and low tritium level in the fluoride-rich groundwater, indicate the effects of long-term of water-rock interactions and intensive evapotranspiration.

Keywords: High fluoride groundwater; Hydrochemical characteristics; water–rock interaction; Ion exchange; **E**vapotranspiration.

1 Introduction

Fluoride concentration is an important aspect of hydrogeochemistry, because of its great impact on human health. The World Health Organization (WHO, 2011) recommends that the highest permissible fluoride content in drinking water should be 1.50 mg L^{-1}.[1] Higher concentrations of this element in drinking water can lead to serious health problems. Therefore, evaluating the causes for the elevated fluoride concentrations is important for a better management of fluoride-rich groundwaters. Many geochemical studies have been performed on various aspects of fluoride in groundwater in recent years. Fluorine is a lithophile element with atmophile affinities, and occurs in many common rock-forming minerals.[2] It has an ionic radius very similar to that of hydroxyl ions, and readily substitutes them during magmatic differentiation.[3] Due to its high partitioning coefficient for low temperature minerals, fluoride can enter into silicate minerals at later stages.[3] Potential sources of fluoride in groundwater include various minerals in rocks and soils, such as topaz ($Al_2(F,OH)SiO_4$), fluorite (CaF_2), fluorapatite ($Ca_{10}(PO_4)6F_2$), cryolite (Na_3AlF_6), amphiboles and micas.[4-6] Fluorite has generally been considered a dominant source of fluoride in groundwater.[7-8] Fluorine is leached into circulating groundwater by mineral weathering. Probably one of the reasons for high F^- content in the groundwater samples is the high mobility of F^- ion due to its small ionic radii, maximum electro-negativity and fairly high mobility.[2] The proportions of F-rich minerals are generally high in granitic rocks relative to other minerals.[9-11] Therefore, high fluoride groundwater often occurs in hard rock areas, particularly those of granitic

composition in different parts of the world.[11-13] In addition, some high fluoride sedimentary aquifer systems derived from granitic parent rocks have been found.[14-15]

Factors responsible for fluoride enrichment in aquifers include geological formation, hydrogeological setting, and hydrogeochemical characteristics.[11,14,16-18] Fluoride concentration in groundwater is variable and controlled by the climate, the amount of fluoride in the rock, solubility of fluorine-bearing minerals, the residence time of the water in the aquifers as well as the temperature and pH, presence or absence of ion complexes and colloids, anion exchange capacity of the aquifer material, as well as the hydrochemical facies.[10,19-23] The concentrations of Ca^{2+}, Na^{+}, HCO_3^{-} and OH^{-} as well as certain ionic complexes such as Fe^{3+}, Al^{3+}, B^{3+}, Si^{4+}, Mg^{2+}, and H^{+} may modify fluoride concentrations.[22-23] The amount of fluoride from fluorite dissolution in waters of low ionic strength is about 8 – 10 mg L^{-1}.[22, 24]

Serious human health problems due to long term intake of high fluoride groundwaters have been reported in China, India, Korea, Pakistan, Mexico, and several countries in Africa.[2-3, 11, 22, 24-29] According to official statistics, 50.85 million people in rural areas of north China drank high fluoride (> 1.5 mg L^{-1}) water in 2005.[30] Groundwater is the most important source for domestic, agricultural, and industrial demands in Datong Basin. Issues of dental and skeletal fluorosis present serious health concerns in the Datong Basin, northern China (Fig. 1). There are 171,760 people living in Shanyin county and Yingxian county, the most seriously fluorosis-affected areas in Datong basin, 82,095 and 8,620 people, respectively, are suffering from severe dental and skeletal fluorosis according to a report.[31] The maximum fluoride concentration in Shanyin County reaches up to 10.35 mg L^{-1}.[17] Mitigation measures have been implemented in some areas of Datong Basin, including provision of piped low-fluoride groundwater from basin margins and use

of small-scale reverse osmosis facilities for defluoridation. However, the effect of the mitigation efforts is still far from solving the serious problems of endemic flurosis at Datong. During the past 10 years, many drinking water supply wells in villages affected by fluorosis have been abandoned. However, many domestic and irrigation wells are still in use, as an alternative water supply option.

The hydrochemical characteristics of high fluoride groundwaters and the factors influencing F levels in sedimentary aquifers in Datong Basin have been investigated in our previous study.[17, 32] The hydrochemical data suggests that the dominant geochemical processes occurred in the study area include silicate weathering and hydrolysis, precipitation and/or dissolution of carbonate, gypsum, and halite together with evapotranspiration. High fluoride groundwaters contains elevated ions concentration, and are of transitional hydrochemical types, with lower Ca^{2+}, and higher HCO_3^- and Na^+.[32] Studying the genesis of soda waters provides new insights into mechanism of fluoride enrichment in the aquifer system. Due to CaF_2 solubility control and OH^--F^- exchange reaction, Na-predominant alkaline environments like soda water are favorable for fluoride enrichment. [17] But the geochemical controls on fluoride enrichment in sedimentary aquifers have not been well understood. In this study, the integrated results of hydrogeochemical and isotopic investigation would be helpful in understanding the mobilization and enrichment mechanisms of F^- in the Datong Basin and the commonly occurring geochemical processes in endemic fluorosis-affected areas of similar sendimentary basins globally.

2 Hydrogeological setting

Datong Basin is one of the Cenozoic faulted basin of the Shanxi rift system,[33] with an area of approximately 6000 km^2. The study area is located in the East Asia monsoon region, with

semi-arid climate. The average precipitation is between 225 mm and 400 mm (mostly during July and August), evapotranspiration above 2000 mm, and the yearly average air temperature 6.5^{o}C.

Datong Basin is surrounded by mountains and the topography slopes down from northwest to southeast. The rivers in the area are ephemeral. The major river, the Sanggan River, runs across the study area from south to north (Fig. 1). Outcrops of the bedrock are observed in the northern, western, and eastern parts of the study area. The outcroppings are Archean gneiss and basalt in the north, Cambrian-Ordovician limestones and Carboniferous–Permian–Jurassic sandstones and shale in the west and Archean gneiss and granite sparsely in the northeast.[17] Scattered around the basin are early Tertiary basalt, late Tertiary laterite soil and early–middle Pleistocene basalt. Cenozoic sediments, with thicknesses between 50 m and 2500 m, are accumulated in the basin. The grain size of sediments generally decreases from the margin to the central area of the basin. The sediments underlying the central part of the basin are a heterogeneous series of laterally discontinuous alluvial-pluvial sands, sandy loam soils and silts, lacustrine and alluvial-lacustrine sandy loam soils, silty clay and clay rich in organic matter.

Fig. 1

Groundwater mainly occurs in the Quaternary alluvial, alluvial-pluvial and alluvial-lacustrine aquifers, which are primarily recharged vertically by infiltrating meteoric water in the basin range and laterally by fracture water from bedrock along the mountain foot. The second recharge source ts the infiltration from non-perennial rivers and irrigation return flow. In general, the recharge of the shallowest unconfined aquifers occurs across the whole basin region. The deeper semi-confined and confined aquifers can only be recharged through the overlying units; this may occur at the basin margins where the coarse surface sediments occur.

Due to limited recharge and the low permeability, groundwater flow is very slow in the low flat terrain and, especially, in the deep aquifers. The velocity of the groundwater movement varies from 0.20 to 0.58 m d^{-1}.[34] Discharge occurs mainly via evapotranspiration and artificial abstraction. There are two major flow paths in regional aquifer system: 1) the one from the mountain foot areas to the central parts of the basin, and 2) the other along Sanggan River from SW to NE in the basin.[34]

3 Sampling and analytical methods

70 groundwater samples were collected from tubewells with depths between 3.5 m and 129 m at Datong basin in September, 2008 (Fig. 1). 29 groundwater samples were selected for hydrogen and oxygen isotope analysis, and 16 samples for tritium.

Before collection, the wells were pumped for more than 5 minutes to flush out the stagnant residual water from the borehole, and the sample bottles were rinsed with analytical grade HCl (2%) and deionized water, respectively. Then, samples were filtered through 0.45 μm membrane filters, and collected into three new 500-mL polyethylene bottles after rinsing with the sample water. Sub-samples for cation analyses were stored in polyethylene bottles and acidified to pH < 2 by addition of 6 M reagent-quality HNO_3. Temperature, pH, and electrical conductivity (EC) were measured on site using portable Hanna EC and pH meter which were calibrated each day before use. Alkalinity was measured by Gran titration using 0.05 N HCl solution on the same day of sampling. Major anions were determined using ion chromatography (DX-120), major cations by ICP-AES (IRIS INTRE Ⅱ XSP type) , and trace metal elements by ICP-MS with a detection limit of 1 μg L^{-1} for most elements. Major ions and trace elements were analyzed within 2 weeks

after sampling. Analytical precision and accuracy were estimated as better than 5% for both major ions and trace metal elements on the basis of repeated analyses of samples and standards. Charge balance errors of all water samples were less than 5%.

Stable isotopes δ^2H and $\delta^{18}O$ of 29 groundwater samples were measured by MAT251. The precisions of δ^2H and $\delta^{18}O$ measurements were ±1 and ±0.1‰ (2σ criterion), respectively. Tritium content of 17 groundwater samples was measured using a Quantulus 1220 liquid scintillation counter proceeded by electrolytic enrichment.[35] The precision of tritium measurements was 0.5 TU (3σ criterion), where 1 TU is 1 atom of tritium in 10^{18} atoms of hydrogen. The chemical and isotopic data in the study area are given in the Table 1.

Table 1

4 Results and discussion

4.1 Hydrogeochemical characteristics

Groundwater hydrochemistry is essential to understand the extent to which the groundwater has interacted with various aquifer minerals and undergone changes in chemical composition. The average of fluoride concentrations is up to 2.2 mg L^{-1} in groundwater, and ranging from 0.1 to 8.26 mg L^{-1} (Table 1). The pH values of groundwater are neutral to moderately alkaline (7.0 to 8.8). The electrical conductivity (EC) and total dissolved solids (TDS) contents are in the range of 316–71,600 μS cm^{-1} and 305.7-8,069 mg L^{-1}, respectively (Table 1), indicating that the groundwaters in the study area are fresh to saline, and most of the samples are brackish in nature.

Figure 2 shows the variation of F^- concentration in groundwater samplers collected from the study area. High F^- levels are shown in the central parts of the basin along the Sanggan River, up

to 8.26 mg L^{-1}. The elevated F^- concentrations mainly occur in the aquifer 3.5 m to 50 m deep.[15]

Fig. 2

F^- concentration is largely controlled by groundwater chemistry. Higher concentration of TDS can enhance the ionic strength, leading to the increase in the solubility of F^- ions in the groundwater.[36] Therefore, high F^- concentration often occurred in high TDS groundwater. Previous study showed that from the mountain front to the central part of basin, EC and TDS in groundwater tend to increase.[32] It can be seen from figure 3a, the average values of other major ions in high F^- groundwater (fluoride concentrations above or at the drinking water standard of 1.5 mg L^{-1} proposed by WHO in 2011) are all higher than those in low F^- groundwater (fluoride concentrations lower than the drinking water standard of 1.5 mg L^{-1} proposed by WHO in 2011).

Groundwater with high F concentrations in the study area has a distinctive major ion chemistry, being generally HCO_3^--rich, Na-rich, Ca-poor and having relatively high pH values (>7.2). The hydrochemical types in the Quaternary aquifer are dominantly HCO_3-Na water (Na^+ made up >47% of total cations; HCO_3^- made up >46% of total anions, Fig. 3), although some high F^- groundwater samples belong to $HCO_3 \cdot SO_4$-Na·Mg, $HCO_3 \cdot Cl \cdot SO_4$-Na·Mg and $SO_4 \cdot Cl$-Na·Mg water.[32] Figure 3b shows that the average molar equivalent percentage of Ca^{2+} and Mg^{2+} in high F^- groundwater are lower than those in low F^- groundwater, while SO_4^{2-} and Cl^- elevated. Due to fluorite solubility control, lower concentrations of Ca^{2+} are favorable for the enrichment of fluoride in groundwater. These data indicate that variations in the groundwater major ion chemistry and possibly pH, which are controlled by water-rock interaction processes in the aquifers are important in mobilizing F^- in the aquifers.

Fig. 3

4.2 Primary source of fluoride

Because the primary source of fluorine is geogenic and its solubility in fresh water is low,[37] fluoride concentrations frequently are proportional to the degree of water–rock interaction.[19,38] Outcropping bedrocks in the study area include granite, gneiss, sandstones and shale, which are comprised of fluoride-bearing minerals like biotite, fluorite and fluorapatite. Climatic conditions such as semi-aridity and high temperature, favor effective chemical weathering of these rocks, which facilitated fluoride mobilization and migration from mountains into basin area. So, fluoride-bearing minerals in granite and gneiss in the subsurface provide a significant source of fluoride in groundwaters.

The primary rock-forming minerals of host rocks in the Quaternary aquifers at Datong Basin are silicates and alumino-silicates.[17] During the processes of hydrolysis, these minerals along with chemical species like Na^+, K^+, F^-, etc., are released into sedimentary aquifers, resulting in the increase in TDS along the groundwater flow paths. A gradual mineralization with changing chemical facies is observed in groundwater along the flow path.[32] It was reported that fluoride is predominant in clay fractions, whereas sand and silts are enriched with much less fluoride.[39] Fluoride–hydroxyl exchange/adsorption reaction occurs in the clay minerals with the alkaline water releasing fluoride into the groundwaters.[40]

Lithogenic sodium (LNa) is the net sodium acquired by groundwater from chemical weathering of rock forming minerals only.[41] The value of LNa is calculated on the basis of chloride [Cl^-] concentration using the formula LNa = [Na^+] – [Cl^-]. The evaluation of LNa is valuable to infer the contribution of Na^+ in the groundwater from the weathered rocks.[28,40] A plot

of LNa versus F^- is supportive for assessing the contribution of F^- from the weathering of albite and other Na-bearing minerals with some influence of ion-exchange.[3] Figure 4a shows close correlation between LNa and fluoride in groundwater samples (r^2=0.807) (sample data in groups (a) and (b) were not included to plot the regression line), reflecting that F^- in the groundwater is mainly acquired from the weathering of parent rocks, and water–rock interaction is the governing process for the F^- leaching.[3] Besides weathering, samples with high F^- in group (b) (sample nos. SHY05, SHY09, SHY12, SHY16, SHY18, SHY19 and SHY27) indicate that there are other sources of fluoride (such as fluoride-bearing fertilizers and ion-exchange), whereas low F^- in samples falling in group (a) (sample nos. SHY22, SHY40, SHY48, SHY49, SHY55 and SHY66) is probably due to removal of F^- from groundwater by different mechanisms like fluorite re-precipitation or inclusion of fluoride in concretions.[3, 40] Considering intensive agricultural activities in the study area, the six groundwater samples with high-fluoride concentration might be partly related to anthropogenic activity such as the use of phosphate fertilizer containing fluoride and pesticides. The weak positive correlation between F^- and NO_3^- concentrations, which are related to agricultural activities, also indicates that input from agricultural chemicals is likely to be a potential F source on a regional scale (Fig. 4b).

Fig. 4

Several trace elements in groundwater can also elucidate their genetic affiliations.[42] The correlation matrix between F–Na, F–Mg, F–Li, F–B, F–Cu, F–Ni, F–Se and F–U reflect that fluoriferous groundwater originates from the weathering of rocks.[3] High content of Li in association with F^- can be considered as evidence of granite–water interaction.[22] Good correlation between Li–F^- (r = 0.69) and Li–Sr (r = 0.68) in the groundwater of study area reflect the

relationship with granite (Table 2). Similarly good correlations between Li, Ni, Cu, Se, U, Sr, B and K, Na, Ca Mg and F^- (+>0.48) indicate association with igneous rocks (Table 2).

Table 2

Log_{10}TDS and Na/Na+Ca ratio[43] of the groundwater is useful to reveal the impact of geochemical processes on hydrochemistry in Datong Basin. Figure 6 shows that the samples were clustered in a zone dominated by weathering process with the influence of evapotranspiration (Fig. 5). The contents of Cl^- with reference to other anions of the groundwater imply weathering as one of the dominant processes.[3] The averaged Cl^-/Σanions ratio in the groundwaters of the study area was 0.217, indicating the influence of rock weathering.

Fig. 5

4.3 Process of water–rock interaction

Leachability of fluoride from the aquifer minerals is mainly controlled by pH and dissolved CO_2 in groundwater.[4] Previous study showed that, compared with low F^- groundwater, high F^- groundwater tends to have weak lower pH, which is ranging from 7.2 to 8.2, although the correlation is not apparent.[15]. According to Guidry and Mackenzie (2003)[44], the dissolution of fluorapatite decreases with the pH values increase. Furthermore, the F^- leaching experiments from biotite by Chae et al. (2006) showed a negative correlation between pH and F^- concentration[42]. This indicates that the F^- leaching from mica primarily associated with mineral weathering, and the role of F^- exchange with OH^- at high pH seems to be minor in increasing the F^- concentration. High pH may also cause de-sorption of F^- from clay minerals surfaces[45-46].

On the other hand, at alkaline pH conditions, calcite precipitation is generally enhanced, which enables further dissolution of fluorite by common ion effect, especially when the

groundwater is saturated with fluorite and calcite at the same time[46]. The preferential removal of Ca^{2+} by several geochemical processes in aquifers, such as calcite precipitation, adsorption and cation exchange, may generate high concentrations of fluoride in groundwater[42]. Our previous study showed that HCO_3^- concentrations increased from the basin margins to its interior, along with increasing Na/Ca ratios[32], while HCO_3^-/anions ratios tend to decrease. In the study area, except for a few of samplers, the majority of groundwater samplers are supersaturated with respect to calcite (S.I. values from -0.58 to +0.96) (Fig. 6) which promotes the removal of Ca^{2+} from solution, indicating that calcite dissolution probably largely occurred during recharge.[47] As a result, the groundwater samples are generally undersaturated with respect to fluorite (CaF_2) (S.I. values from -3.70 to +0.56). These suggest that fluorite dissolution may have occurred while not the second-stage calcite dissolution under closed system conditions, to maintain calcite equilibrium after cation exchange lowered the Ca^{2+} content.[46] In other words, fluorite dissolution in study area is enhanced by the ongoing process of calcite precipitation.

Formerly, solubility control of fluorite has been considered as the main geochemical barrier for fluoride concentration in most environments.[24] Fig. 6 shows that the groundwaters approach to be saturated with respect to fluorite, along with increasing F^- content, indicating that fluorite dissolution probably occurred for elevated F^- groundwater. In addition, some previous studies also have proposed that F concentration can be increased even when the water is saturated with fluorite due to common ion effect with calcite precipitation.[15, 24] Therefore, other geochemical factors may also restrict fluoride concentration from increasing in groundwater besides solubility control of fluorite.

Fig. 6

According to Kim et al. (2012)[46], both the common ion effect and high pH may be

dominating controls, and cation composition is likely the more important factor. However, it is difficult to completely separate the influence of cation composition and pH, as the Na-rich groundwater generally has higher pH. In addition, much of the HCO_3^- in groundwater derives from weathering of carbonate minerals during recharge and to some extent in the aquifer matrix[47], meaning that pH and HCO_3^- concentrations are also partly linked, as carbonate weathering increases both parameters, particularly under closed system conditions (e.g. Clark and Fritz, 1997)[48]. Therefore, pH alone does not seem to be a dominant factor controlling F^- enrichment.[15]

A positive correlation between HCO_3^- and F^- with regression coefficient of 0.63 was shown in Fig. 7, in which sample data falling in groups (a) and (b) were not considered for plotting regression line. Samples falling in group a (sample numbers: SHY22, SHY40, SHY48, SHY49 and SHY66) have low F^- and high HCO_3^- concentrations. This is because that they were sampled from the wells with depths greater than 43 m where reducing conditions prevail. Group (b) samples (sample nos. SHY05, SHY09, SHY11, SHY12 and SHY16) show high F^- and low HCO_3^- concentrations. This could be due to fluoride contribution from other sources such as fluoride-bearing fertilizers or high fluoride unconfined aquifers, in addition to weathering. This correlation indicates that high HCO_3^- content in groundwaters facilitates fluorite dissolution in Datong Basin. The result is consistent with other studies,[49-50] which showed elevated alkalinity tend to mobilize F^- from weathered rocks and sediments, and release F^- from CaF_2 with the simultaneous precipitation of $CaCO_3$.

Fig. 7

The elevated fluoride contents in the groundwater is also linked to ion exchange, which causes the removal of Ca^{2+} from the solution by replacing with Na^+ in aquifer matrixes due to

sluggish movement of groundwater.[32,48] A plot of log TDS versus $Na^+/(Na^+ + Cl^-)$ can be used to suggest the process of ion exchange whether is occurring or not within the study area.[3] On Fig. 8, except for four samples with high F^- (>1.5 mg L^{-1}) content plotted within the reverse softening field, the majority of groundwater samples with high (>3 mg L^{-1}) F^- concentrations within the ion exchange field. This demonstrates the water softening process occurred in the groundwater, which can influence the mobility of F^-.

Fig. 8

The sodium absorption ratio (SAR) used to express sodium hazard is calculated by the formula:

$$\mathrm{SAR} = \frac{[Na^+]}{\sqrt{([Ca^{2+}]^2 + [Mg^{2+}]^2)/2}}$$

High Na^+ in groundwater mainly originates from the dissolution of LNa and the exchange of dissolved Ca^{2+} for Na^+ by clay minerals in the aquifer. Figure 9a shows that the calculated values of SAR tend to increase with F^- concentrations. The average value of SAR in high F- groundwater (> 1.5 mg L^{-1}) (with a value of 3.00) is higher than that in low F^- groundwater (< 1.5 mg L^{-1}) (with a mean value of 1.95).

Fig. 9

The calculated $Ca^{2+}/(Ca^{2+} + SO_4^{2-})$ ratios in high groundwater range from 0.02 to 0.71 (with a mean value of 0.32) (Fig. 9b), which provide additional support for the process of ion exchange.[51] Figure 9b shows a strong negative correlation between F^- concentration and $Ca^{2+}/(Ca^{2+} + SO_4^{2-})$ ratio. It was reported that the groundwater Ca^{2+} content would still remain low under this scenario provided that there was still exchangeable Na^+ to allow cation exchange to continue.[52] Due to limited recharge and the low permeability, groundwater flow is very slow in the study area. The

environmental tritium content of most of the samples is in the range of 1.5 to 2.1 TU, except for sample SHY44 with the value 1.07 TU (Table 3). Low tritium values (<2.5 TU) indicate old ages and long residence time of groundwater. These results may explain the general observation that high fluoride concentration in sedimentary aquifers is usually associated with Ca-poor and Na-rich groundwater.

Table 3

4.4 Evapotranspiration

Isotope approach

Although hydrochemical data analysis indicated that interaction of alkaline waters with sediments is responsible for fluoride enrichment in groundwaters, the effect of evapotranspiration should not be neglected in such an arid region like Datong. Hydrogen and oxygen isotopes may provide clues about the effect. Results of stable isotope composition analysis reveal that the groundwaters from Datong Basin are isotopically fractionated by evapotranspiration and/or water–rock interactions. A gradual enrichment in stable isotopes is observed in along the groundwater flow-path. $\delta^{18}O$ in groundwater increase away from the basin margins, towards the central Basin (Fig. 2).

Plot of $\delta^{2}H$ versus $\delta^{18}O$ shows that groundwater samples fall on the line with a lower slope of 3.9, indicating evapotranspiration effects (Fig. 10). The China Meteoric Water Line (CMWL: $\delta D=7.9\delta^{18}O+8.2$) and Taiyuan Meteoric Water Line (TMWL: $\delta D=6.66\delta^{18}O-3.08$) are shown in figure 10 as the reference lines. Taiyuan is the capital of Shanxi province, south of Datong. The simultaneous decreases of $\delta^{18}O$ and δD values in some low F^- groundwater samples reflect the

effect of altitude of recharge. The positive shifts away from the meteoric lines indicate the effect of evapotranspiration, which is also reflected by the almost simultaneous variations in $\delta^{18}O$ and fluoride contents (Fig. 2). From the statistical data, groundwater samples with low F^- concentration have stable isotopic values $\delta^{18}O$ between −8.33 and -12.52‰ and $\delta^{2}H$ values ranging −91.6 to −70.3‰, while high F^- groundwater samples have stable isotopic values $\delta^{18}O$: -6.65 to -12.21‰ and $\delta^{2}H$: −84.1 to -56.9‰. High fluoride groundwater samples had much heavier δD and $\delta^{18}O$ values (mean -73.6‰ and -9.4‰ respectively) than low fluoride groundwater samples (mean -83.8‰ and -11.2‰ respectively).

Fig. 10

It was reported that high F^- concentrations in groundwater in arid and semiarid regions may be resulted from the condensation of soluble components due to evaporation and evapotranspiration.[14, 25] The groundwater with low-fluoride concentration was mainly distributed at relative low δD and $\delta^{18}O$. The majority of groundwater samples with high-fluoride concentrations were distributed at high δD and $\delta^{18}O$, throughout relative wide δD and $\delta^{18}O$ ranges (Fig. 10), again confirming that high-fluoride concentrations were affected by evapotranspiration. As shown in figure 10, fluoride concentration first increased gradually, and level off until the values of δD and $\delta^{18}O$ close to the average values (mean -73.6‰ and -9.4‰ respectively) in high fluoride groundwater samples. This suggests that although evapotranspiration is favorable for F^- enrichment in groundwater, F^- in groundwater cannot be enriched infinitely with excessive evapotranspiration. Our previous study showed if evaporation were too strong, MgF_2 might begin to precipitate because of rather high Mg^{2+} concentration.[15]

Fig. 11

Because evapotranspiration should have concentrated Cl^- and F^- equally, the high F^-/Cl^- ratios indicate that enrichment of fluoride is independent of evapotranspiration, as only a few groundwater samplers are saturated with respect to fluorite. However, most of high saline groundwaters (TDS > 2000 mg L^{-1}) have rather elevated F^- concentrations and relatively low F/Cl ratios (Fig. 11), indicating that evapotranspiration does contribute to the high F concentrations, particularly in the aquifers occurred locally with shallow depths.

5. Conclusions

Hydrogeochemical investigation indicates that fluoride concentrations range from 0.1 to 8.26 mg L^{-1} in groundwater of Datong Basin, and tend to increase along with the regional groundwater flow path from the margin to the central area of the basin. Groundwater with high F concentrations has a distinctive major ion chemistry, being generally HCO_3^--rich, Na-rich, Ca-poor and having relatively weak alkaline pH values (7.2 to 8.2). These data indicate that variations in the groundwater major ion chemistry and possibly pH, which are controlled by water–rock interaction processes in the aquifer, are important in mobilizing F.

The origin of fluoride is mostly from the weathered granite and granitic gneiss. The constituents of groundwater such as Na^+, K^+, Mg^{2+}, B, Li Ni, Cu, Se, U, and Sr mainly originate from water-rock interaction. Positive correlations between fluoride with LNa and HCO_3^- in groundwater show that the high fluoride content and alkaline sodic characteristics of groundwater result from dissolution of fluorine-bearing minerals. The occurrence and behavior of fluorine in groundwater are mainly controlled by fluorite precipitation as a function of Ca^{2+} concentration which depends on several geochemical processes such as dissolution of Ca-bearing minerals,

calcite precipitation, and cation exchange. High fluoride groundwater samples contain elevated δD and $\delta^{18}O$, low F^-/Cl^- ratios, and the presence of low tritium reflecting the effects of long water–rock reaction and evapotranspiration.

Acknowledgements

The research work was jointly supported by National Natural Science Foundation of China (Nos. 40802058) and the Ministry of Science and Technology of China (2012AA062602). The authors would like to appreciate the reviewers and editors for their helpful comments and suggestions.

References

1 WHO (World Health Organization), *Guidelines for Drinking-Water Quali*ty, Geneva, 2011.

2 T. Rafique, S. Naseem, T. H. Usmani, E. Bashir, F. A. Khan and M. I. Bhanger, *J. Hzazrd. Mater*, 2009, **171**, 424-430.

3 S. Naseem, T. Rafique, E. Bashir, M. I. Bhanger , A. Laghari and T. H. Usmani, *Chemoshpere*, 2010, **78**, 1313-1321.

4 B. K. Handa, *Groundwater*, 1975, **13**, 275-281.

5 A. Bardsen, K. Bgorraton and K. A. Selving, *Acta Odontol. Scand.*, 1996, **54**, 343-347.

6 R. N. Subba and D. J. Devadas, *Environ. Geol.*, 2003, **45**, 243-251.

7 A. N. Deshmukh, P. M. Valadaskar and D. B. Malpe, *Gondwana Geo.l Mag.*,1995,**35**, 1-20.

8 M. T. Shah and S. Danishwar, *Environ. Geochem. Health*, 2003, **25**, 475-481.

9 J. C. Babiley, *Chem. Geol.*, 1977, **19**, 1-42.

10 K. Kim and G. Y. Jeong, *Chemosphere*, 2005, **58**, 1399-1408.

11 Y. Kim, J. M. Kim and K. Kim, *Environ. Earth Sci.*, 2011, **63**, 1139-1148.

12 W. M. Edmunds and P. L. Smedley, in *Essentials of Medical Geology: the impacts of natural environment on public health*, ed. O. Selinus, Elsevier Academic Press, Burlington., 2005, pp. 301-329.

13 G. T. Chae, S. T. Yun, B. Mayer, K. H. Kim, S. Y. Kim, J. S. Kown, K. Kim and Y. K. Koh, *Sci. Total Environ.*, 2007, **385**, 272-238.

14 Q. Guo, Y. Wang, T. Ma and R. Ma, *J. Geochem. Explor.*, 2007, **93**, 1-12.

15 C. Su, Y. Wang, X, Xie and J. Li, *J. Geochem. Explor.*, 2013a, **12**, 79-92.

16 D. Gosselin, J. Headrick, F. Harvey, R. Tremblay and K. McFarland, *Ground Water Monit. Reme.*, 1999, **19**, 87-95.

17 Y. Wang, S. L. Shvartsev and C. Su, *Appl. Geochem.*, 2009, **24**, 641-649.

18 P. Mamatha and S. M. Rao, *Environ. Earth Sci.*, 2010, **61**, 131-142.

19 J. J. Carrillo-Rivera, A. Cardona and W. M. Edmunds, *J. Hydrogeol.*, 2002, **261**, 24-47.

20 D. Sujatha, *Environ. Geol.*, 2003, **44**, 587-591.

21 M. I. Leybourne, J. M. Peter, K. H. Johannesson and D. R. Boyle, *Geol.*, 2008, **36**, 115-118.

22 L. Valenzuela-Vásquez, J. Ramírez-Hernández, J. Yeyes-López, A. Sol-Uribe and O. Lázaro-Mancilla, *Environ. Geol.*, 2006, **51**, 17-27.

23 S. M. Yidana, D. Ophori, B. Banoeng-Yakubo and A. A. Samed, *ARPN J. Eng. Appl. Sci.*, 2012, **7**, 50-68.

24 W. B. Apambire, D. R. Boyle and F. A. Michel, *Environ. Geol.*, 1997, **33**, 13-24.

25 G. Jacks, P. Bhattacharya, V. Chaudhary and K. P. Singh, *Appl. Geochem.*, 2005, **20**, 221-228.

26 P. D. Sreedevi, S. Ahmed, B. Made, E. Ledoux and J. M. Gandolfi, *Environ. Geol.*, 2006, **50**, 1-11.

27 R. Tekle-Haimanot, Z. Melaku, H. Kloos, C. Reimann, W. Fantaye, L. Zerihun and K. Bjorvatn, *Sci. Total Environ.*, 2006, **367**, 182-190.

28 E. Shaji, V. J. Bindu and D. S. Thambi, *Curr. Sci.*, 2007, **92**, 240-245.

29 T. Ayenew, *Environ. Geol.*, 2008, **54**, 1313-1324.

30 National Development and Reform Commission, Ministry of Water Resources, Ministry of Public Health, 2005, 11th Five-year Plan for National Safeguarding Rural Drinking Water Project.

31 J. H. Wang, *Neimenggu Preventive Medicine*, 1997, **22**, 145-147 (In Chinese).

32 C. Su, Y. Wang and Y. Pan, *Environ. Earth Sci.*, 2013b, **70**, 877-885.

33 Y. X. Wang and G. M. Shpeyzer, *Hydrogeochemistry of Mineral Waters from Rift Systems on the East Asia Continent: Case Studies in Shanxi and Baikal(in Chinese with English abstract)*, China Environmental Science Press, Beijing, 2000.

34 X. Xie, A. Ellis, Y. Wang, Z. Xie, M. Duan and C. Su, *Sci. Total Environ.*, 2009, **407**, 3823-3835.

35 A. R. Nair, Proceedings of the Workshop on Isotope Hydrology, Mumbai, 1983.

36 A. I. Perel'man, *Geochemistry of Elements in the Supergene Zone (Translated from Russian)*, Keter Pub, Jerusalem, 1977.

37 D. K. Nordstron and E. A. Jenne, *Geochim. Cosmochim. Acta*, 1977, **41**, 175-188.

38 B. Frengstad, D. Banks and U. Siewers, *Sci. Total Environ.*, 2001, **277**, 101-117.

39 N. Madhavan and V. Subranmanian, *J. Environ. Monit.*, 2002, **4**, 821-822.

40 K. Tirumalesh, K. Shivanna and A. A. Jalihal, *J. Hydrogeol.*, 2007, **15**, 589-598.

41 V. Ramesam and K. Rajagopalan, *J. Geol. Soc. India*, 1985, **26**, 125-132.

42 G. T. Chae, S. T. Yun, M. J. Kwon, S. Y. Kim and B. Mayer, *Geochem. J.*, 2006, **40**, 95-102.

43 R. J. Gibbs, *Sci.*, 1970, **17**, 1088-1090.

44 M. W. Guidry and F. T. Machenzie, *Geochim Cosmochim. Acta*, 2003, **67**, 2949-2963.

45 A. P. Viero, C. Roisenberg, A. Roisenberg and A. Vigo, *Environ. Geol.*, 2009, **56**, 1707-1719.

46 S. Kim, K. Kim, K. Ko, Y. Kim and K. Lee, *Chemosphere,* 2012, **87**, 851-856.

47 M. J. Currell, I. Cartwright, D. C. Bradley and D. Han, *J. Hydrol.*, 2010, **385**, 216-229.

48 S. R. Tamta, *Hhu-Jal News*,1994, **6**, 5-11.

49 N. V. Ramamohana Rao, N. Rao, K. Surya Rao and R. D. Schuiling, *Environ. Geol.*, 1993, **21**, 84-89.

50 V. K. Saxena and S. Ahmed, *Environ. Geol.*, 2003, **43**, 731-736.

51 A. W. Hounslow. *Water Quality Data: Analysis and Interpretation*, CRC Press, 1995.

52 K. Walraevens, J. Cardenal-Escarcena and M. V. Camp, *Appl. Geochem*, 2007, **22**, 289-305.

Fig. 1 Location of the study area and the sampling sites.

Fig. 2 Distrabution of F^- and $\delta^{18}O$ (‰) concentrations in the groundwater.

Fig. 3 Mean values (a) and molar equivalent percentage (b) of major ions in groundwater with different fluoride concentrations

Fig. 4 Scatter plot of lithogenic sodium (a) and NO_3^- (b) versus fluoride. The solid line is the linear fit to the data excluding group (a) and (b). epm equivalents per million, i.e. (ppm × valence) atomic weight. lithogenic Na (epm)= Na(epm)-Cl(epm)

Fig. 5 Groundwater samples from Datong Basin plotted on the graph of Gibbs (1970).

Fig. 6 Scatter plot of calcite saturation index versus fluorite saturation index of groundwater samples with fluoride concentration indicated as bubbles.

Fig. 7 Correlation between HCO_3^- versus F^- concentration in groundwater. Group (a) and (b) indicate samples with low and high fluoride concentrations respectively. The solid line is fitted by the data points excluding group (a) and (b).

Fig. 8 Correlation plot of TDS in groundwater with $Na^+/(Na^+ + Cl^-)$ (epm) with F^- content indicated as bubbles.

Fig. 9 Correlation plot of fluoride concentration with SAR (a) and $Ca^{2+}/(Ca^{2+} + SO_4^{2-})$ ratio (epm) (b) in groundwater.

Fig. 10 Groundwater samples with F^- concentration plotted on the $\delta^{18}O$ and δD plot.

Fig. 11 Correlation plot of F^-/Cl^- (epm) versus F^- concentration of groundwater samples with TDS content indicated as bubbles.

Table 1 Statistics of Physico-chemical parameters of groundwater samples at Datong Basin.

Table 2 Correlation matrix among important pairs of elements in groundwater samples at Datong Basin.

Table 3 Concentrations of major elements in groundwater at Datong Basin.

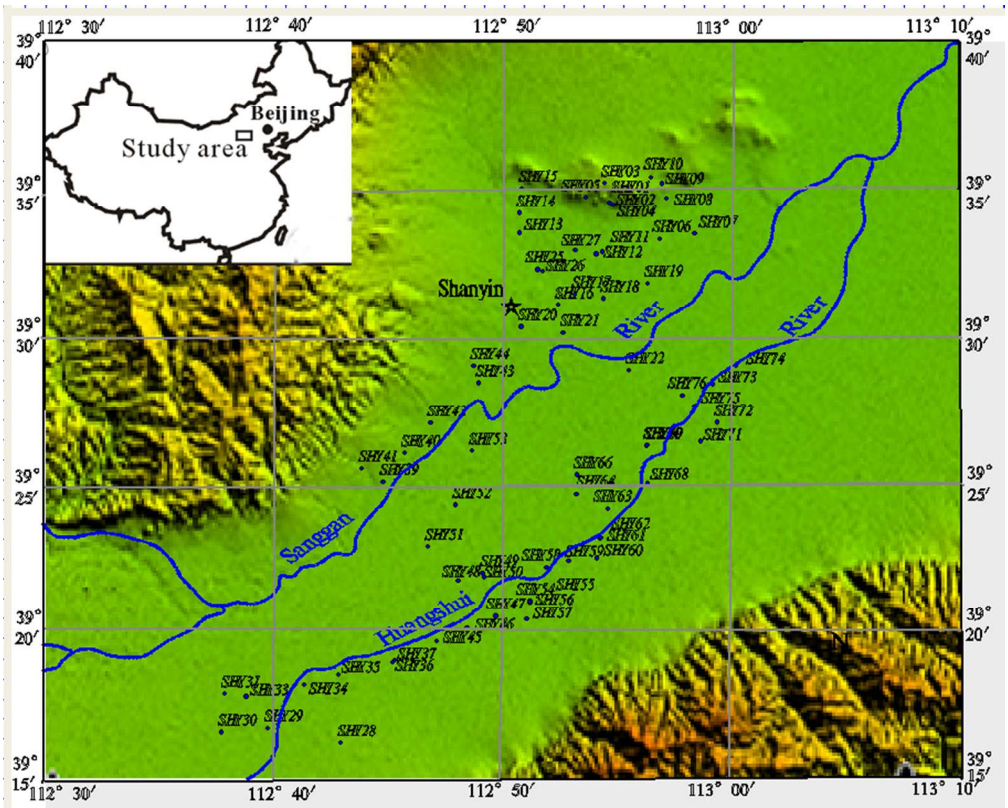

319x256mm (72 x 72 DPI)

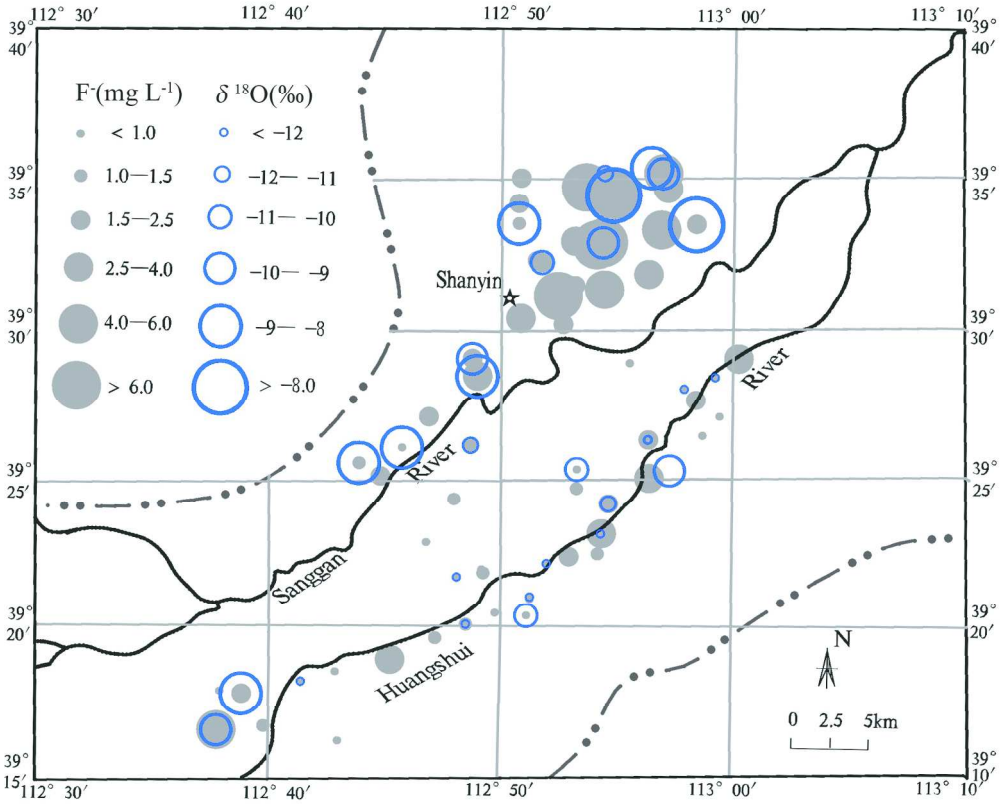

185x151mm (300 x 300 DPI)

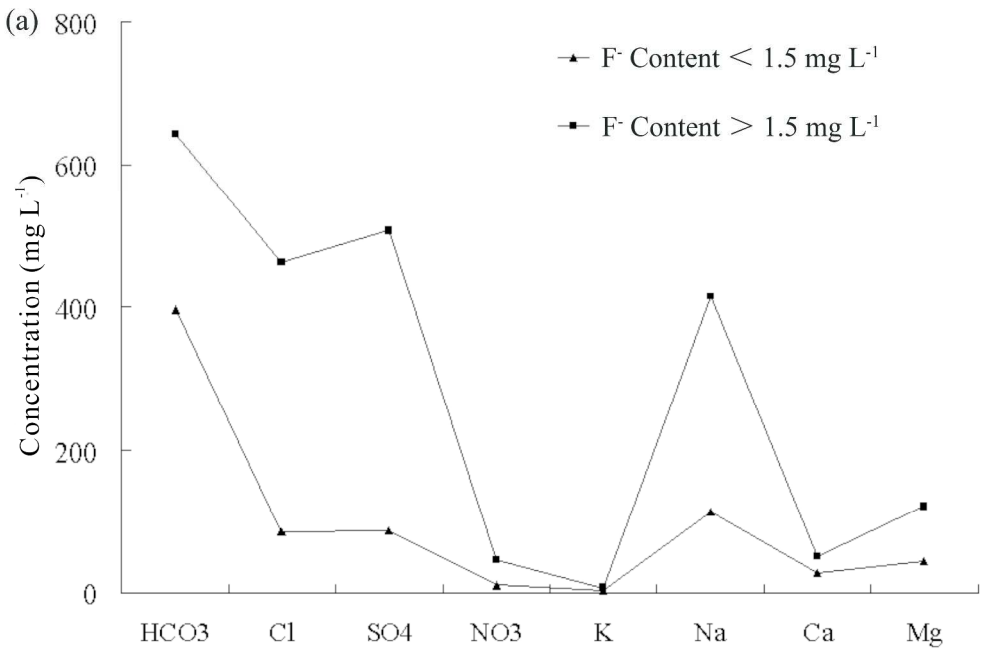

299x223mm (299 x 299 DPI)

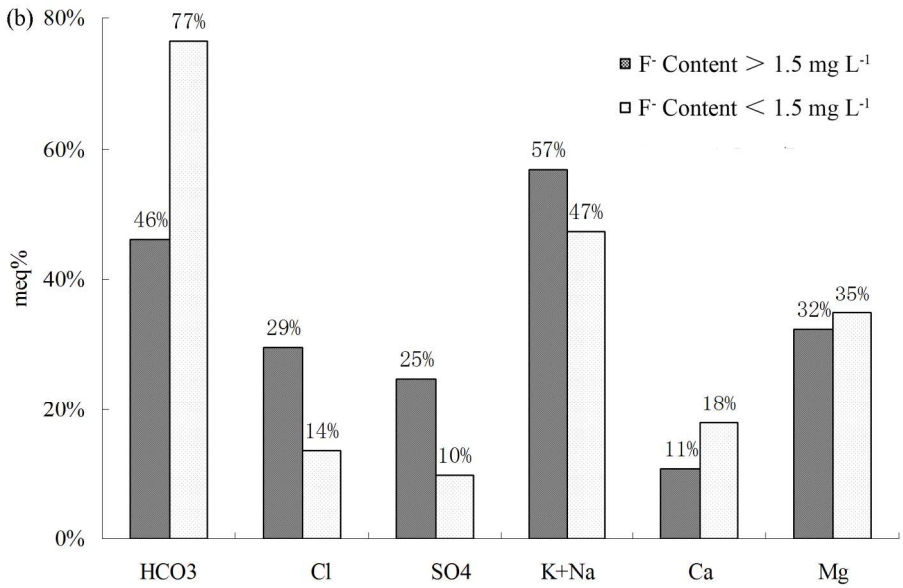

723x464mm (72 x 72 DPI)

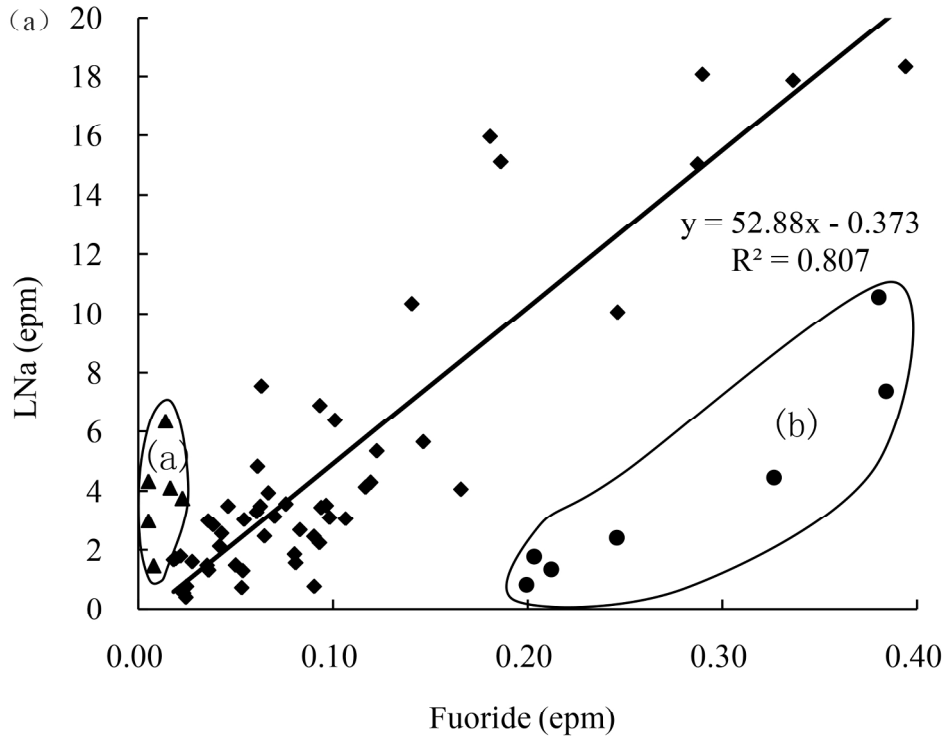

195x171mm (300 x 300 DPI)

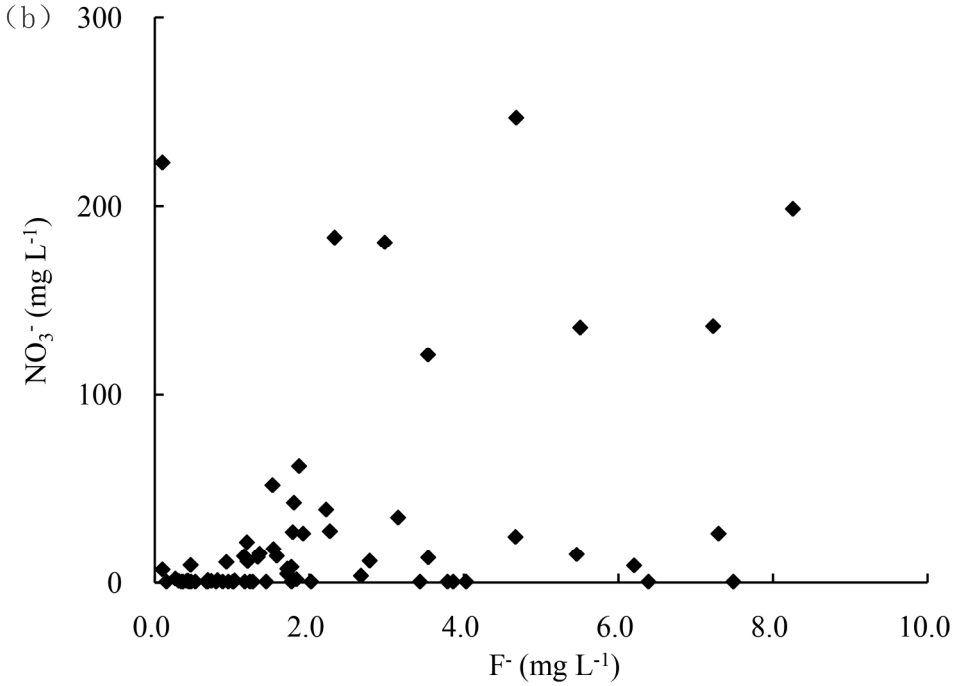

180x145mm (300 x 300 DPI)

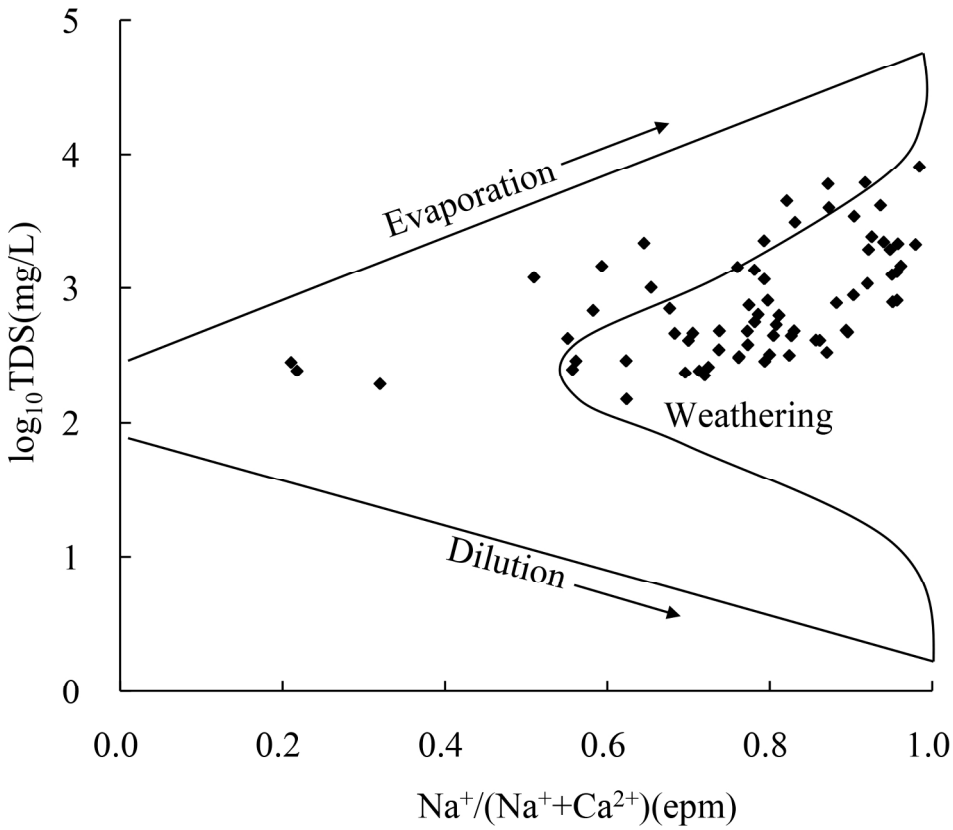

184x171mm (300 x 300 DPI)

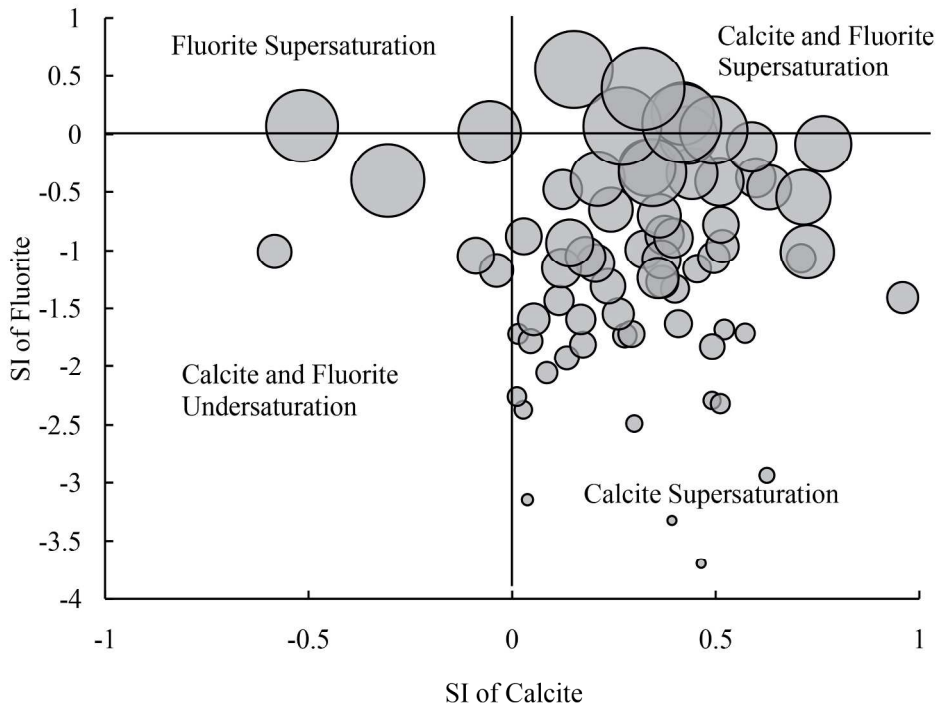

216x171mm (300 x 300 DPI)

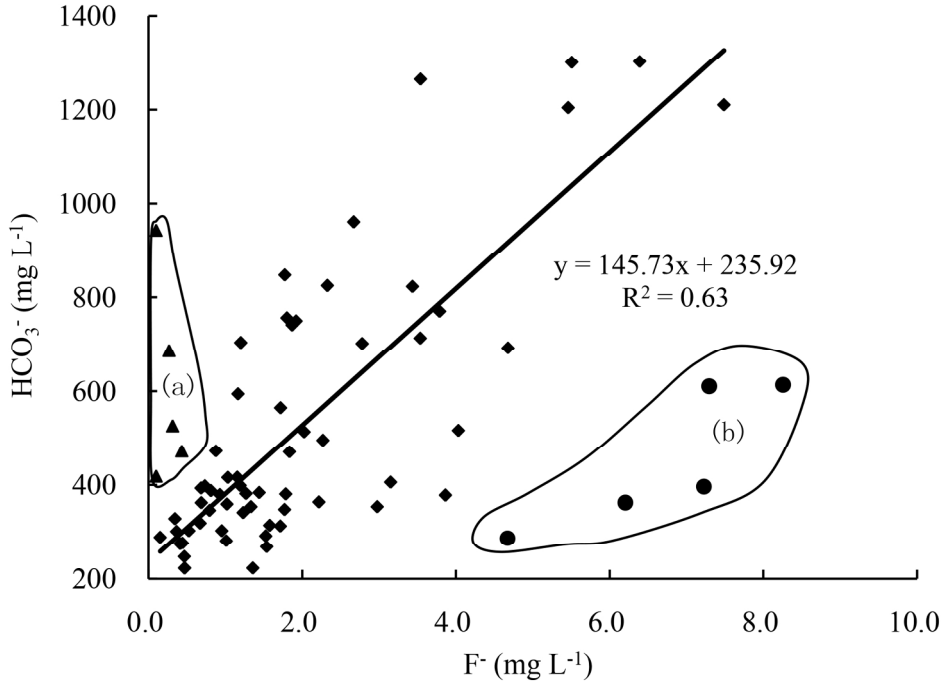

180x139mm (300 x 300 DPI)

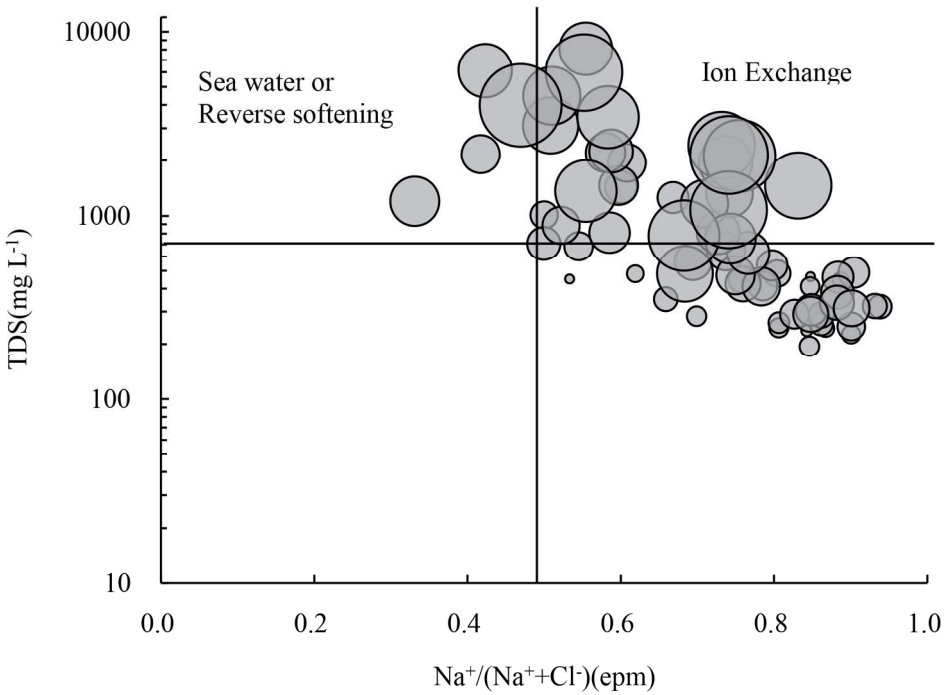

180x141mm (300 x 300 DPI)

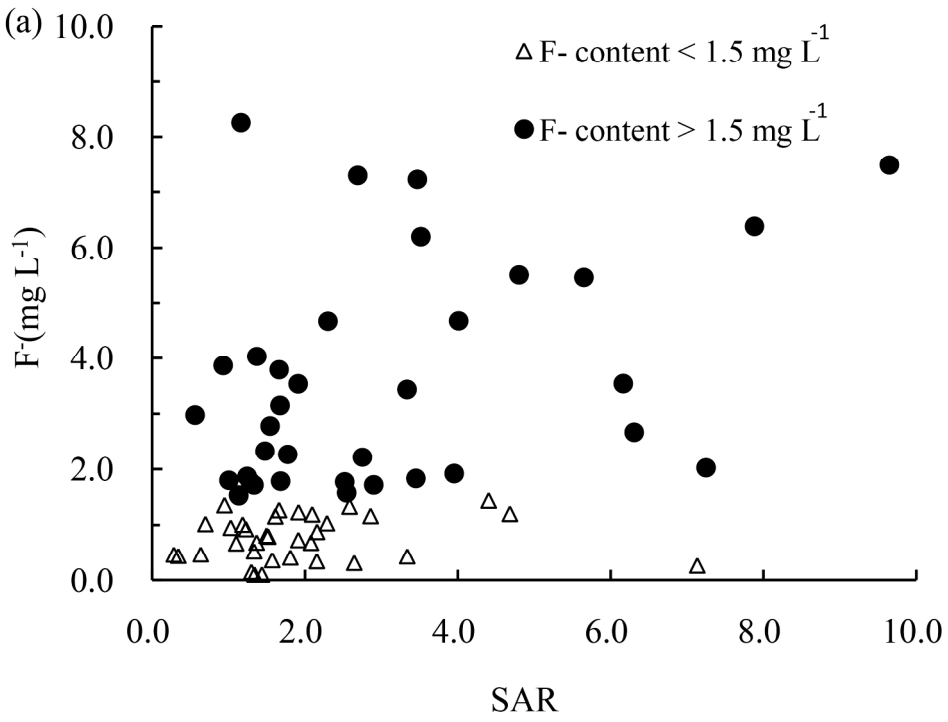

217x171mm (300 x 300 DPI)

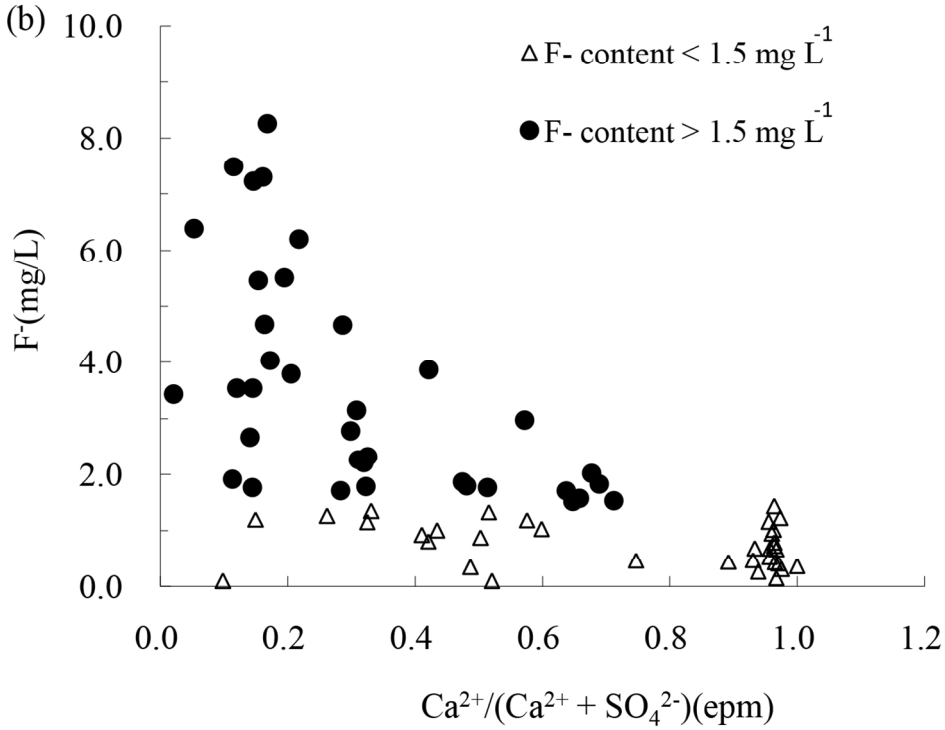

122x96mm (300 x 300 DPI)

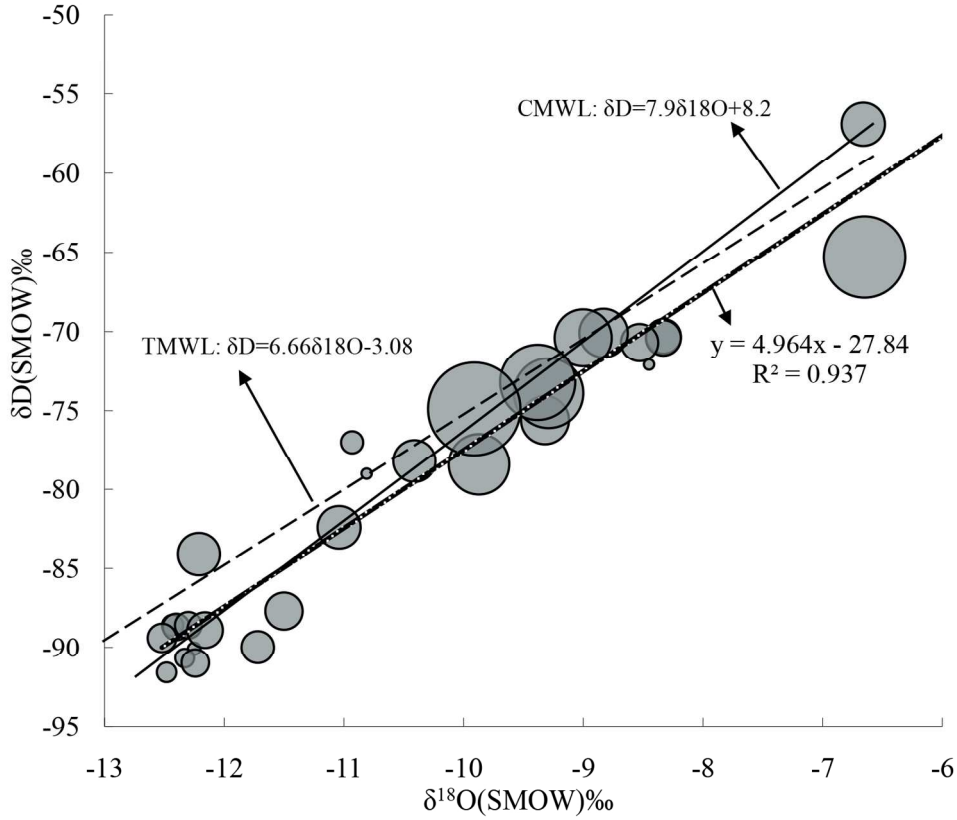

147x130mm (300 x 300 DPI)

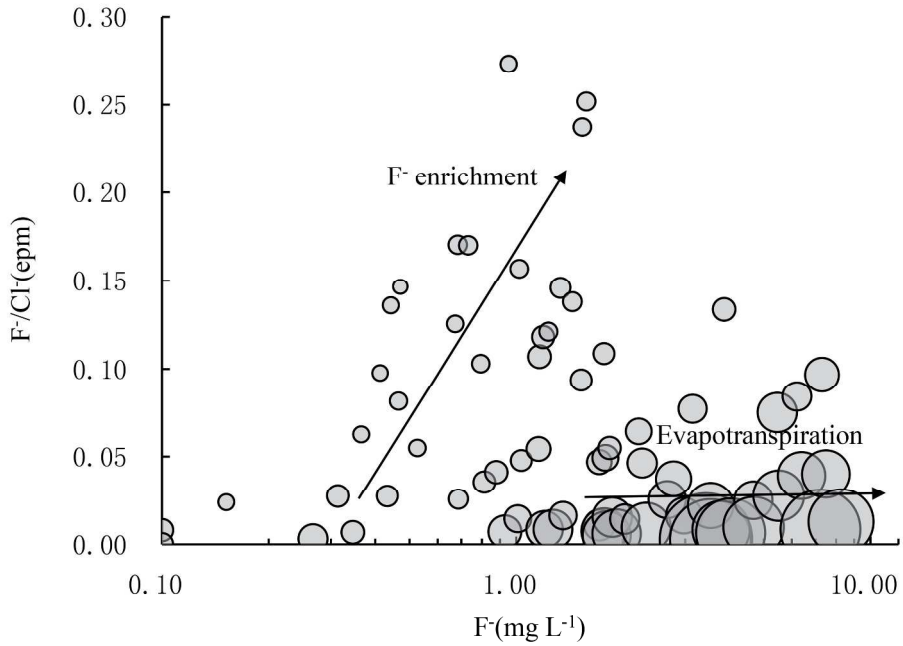

234x171mm (300 x 300 DPI)

Table 1 Statistics of Physico-chemical parameters of groundwater samples in Datong Basin.

Sample No.	pH	Ec	TDS	K^+	Na^+	Ca^{2+}	Mg^{2+}	HCO_3^-	SO_4^{2-}	Cl^-	NO_3^-	F^-	Li	Ni	Cu	Se	U	B	Sr
		μS cm^{-1}	mg L^{-1}	mg L^{-1}	mg L^{-1}	mg L^{-1}	mg L^{-1}	mg L^{-1}	mg L^{-1}	mg L^{-1}	mg L^{-1}	mg L^{-1}	μg L^{-1}	μg L^{-1}	μg L^{-1}	μg L^{-1}	μg L^{-1}	μg L^{-1}	μg L^{-1}
[a]Min	7	316	194.2	0.1	16	9.5	7.3	222	0	6	0.5	0.1	3.45	0.28	2.12	0.40	0.02	0.02	0.25
Max	8.8	71600	8071	65.9	1870	165	437	1303	3000	2400	247	8.3	203.8	5.23	174.0	17.14	97.41	2.30	5.48
Mean	7.9	5211	1274	4.7	268.8	39.7	84.3	523.1	303.6	280.3	28.9	2.2	41.9	1.5	21.8	2.2	19.0	0.5	1.2
S.D.	0.3	11466	1541	10.7	333.1	35.4	107.4	275.2	538.7	485.5	57.4	2.0	40.5	1.2	28.5	2.8	24.8	0.5	1.1

[a]Min: minimal value; Max: maximal value; Mean: mean value; S.D.: Standard deviation.

Table 2 Correlation matrix among important pairs of elements of groundwater of Datong Basin.

	K^+	Na^+	Ca^{2+}	Mg^{2+}	HCO_3^-	Cl^-	SO_4^{2-}	F^-	Li	Ni	Cu	Se	U	B	Sr
K^+	1	0.56**	0.46**	.68**	0.34**	0.58**	0.56**	0.11	0.48**	0.53**	0.54**	0.35**	0.30*	0.50**	0.54**
Na^+		1	0.43**	0.80**	0.58**	0.93**	0.95**	0.57**	0.70**	0.68**	0.98**	0.62**	0.62**	0.76**	0.51**
Ca^{2+}			1	.64**	0.08	0.55**	0.56**	0.33**	0.50**	0.44**	0.37**	0.44**	0.30*	0.16	0.84**
Mg^{2+}				1	0.33**	0.91**	0.86**	0.41**	0.70**	0.61**	0.77**	0.49**	0.43**	0.49**	0.82**
HCO_3^-					1	0.36**	0.34**	0.51**	0.39**	0.69**	0.53**	0.36**	0.68**	0.69**	0.20
Cl^-						1	0.94**	0.45**	0.63**	0.63**	0.91**	0.54**	0.43**	0.56**	0.63**
SO_4^{2-}							1	0.49**	0.72**	0.56**	0.93**	0.60**	0.52**	0.64**	0.60**
F^-								1	**0.69****	0.45**	0.51**	0.51**	0.77**	0.57**	0.46**
Li									1	0.38**	0.67**	0.63**	0.79**	0.61**	**0.68****
Ni										1	0.66**	0.48**	0.51**	0.55**	0.48**
Cu											1	0.62**	0.60**	0.74**	0.44**
Se												1	0.62**	0.57**	0.46**
U													1	0.66**	0.40**
B														1	0.28*
Sr															1

*. significant at 0.05 level.

**. significant at 0.01 leve.

Table 3 Concentrations in major elements for groundwater at Datong Basin.

Sample No.	δD SMOW, ‰	$\delta^{18}O$ SMOW, ‰	^{3}H Bq L^{-1}	Sample No.	δD SMOW, ‰	$\delta^{18}O$ SMOW, ‰	^{3}H Bq L^{-1}
SHY03	-11.5	-87.7	1.98±1.16	SHY46	-12.16	-88.9	1.79±1.10
SHY04	-6.65	-65.3		SHY48	-12.43	-88.6	1.70±1.10
SHY07	-6.66	-56.9		SHY53	-11.72	-90.0	1.59±1.10
SHY09	-9.29	-73.9	1.61±1.10	SHY55	-12.25	-90.1	
SHY10	-8.33	-70.3		SHY57	-10.93	-77.0	1.50±1.10
SHY11	-9.91	-74.9		SHY58	-12.3	-88.6	1.90±1.26
SHY13	-8.53	-70.7	2.10±1.33	SHY61	-12.48	-91.6	1.92±1.33
SHY26	-10.41	-78.2	1.63±1.10	SHY63	-11.04	-82.4	
SHY30	-9.38	-73.2		SHY66	-10.81	-79.0	
SHY33	-8.83	-70.1		SHY68	-9.87	-78.4	
SHY34	-12.33	-90.7	1.55±1.10	SHY69	-12.21	-84.1	
SHY40	-8.45	-72.1	1.66±1.10	SHY70	-12.52	-89.4	1.60±1.10
SHY41	-8.33	-70.4	1.58±1.10	SHY73	-12.24	-91.0	1.57±1.10
SHY43	-9.00	-70.4		SHY76	-12.4	-88.7	1.77±1.23
SHY44	-9.32	-75.6	1.07±1.27				